Development of a User Haptic Feedback Differential Drive

Authors:
Franck Junior Boukila[a]
Nico Steyn[b]
Karim Djouani[b]

Affiliations:
[a]Department of Electrical Engineering, Tshwane University of Technology, South Africa
[b]French South African Institute of Technology, Tshwane University of Technology, South Africa

Corresponding author:
Franck Junior Boukila
E-mail:
franckjboukila3@gmail.com

Dates:
Received: 22/12/20
Accepted: 18/06/21
Published: 19/08/21

How to cite this article:
Franck Junior Boukila, Nico Steyn, Karim Djouani, Development of a User Haptic Feedback Differential Drive, *Suid-Afrikaanse Tydskrif vir Natuurwetenskap en Tegnologie* 40(1) (2021). https://doi.org/10.36303/SATNT.2021.40.1.807

’n Afrikaanse vertaling van die manuskrip is aanlyn beskikbaar by http://www.satnt.ac.za/index.php/satnt/article/view/807

This paper concerns the modelling of a two degrees of freedom motion platform that may be employed in an augmented reality environment for manual mobility aids. The augmented motion platform serves as an evaluation or rehabilitation tool for a lower limb disabled user with their associated manual mobility aid. This manual mobility aid may be seen as a conventional manual wheelchair with a manual propelled differential drive action. The two degrees of freedom associated with the motion platform creates an augmented navigation in a fictitious environment. The two degrees of freedom related to augmented navigation lets the user progress in a fictitious environment and experience haptic dynamic feedback. The produced haptic feedback on the augmented navigation is due to a simulated gravitational force and inertial forces to be experienced by a manual wheelchair user as in reality. It is evident from the above that proper dynamic models of the manual wheelchair and its user on the two degrees of freedom motion platform need to be developed and implemented to create an effective augmented haptic simulated environment.

Keywords: Manual mobility aids, Augmented reality, Haptic feedback, Fictitious environment

Abbreviations

DOF	Degrees of Freedom
LabVIEW	Laboratory Virtual Instrument Engineering Workbench
LQR	Linear Quadratic Regulator
PID	Proportional Integral Derivative
FPGA	Field Programmable Gate Array
ADL	Activity of Daily Living
NI	National Instruments
RIO	Reconfigurable Input Output
COM	Centre of Mass
VSD	Variable Speed Drive
VR	Virtual Reality
AR	Augmented Reality
FOW	Field of View
HMD	Head Mounted Display

Ontwikkeling van differensiële aandrywing met haptiese gebruikersterugvoer: Hierdie artikel handel oor die modellering van ’n bewegingsplatform met twee grade van vryheid wat in ’n geougmenteerderealiteit-omgewing vir handgedrewe mobiliteithulpmiddels aangewend kan word. Die geougmenteerde bewegingsplatform dien as ’n evaluerings- of rehabilitasiehulpmiddel vir gebruikers met ’n gestremde onderste ledemaat en die handgedrewe mobiliteitshulpmiddel wat hulle gebruik. Hierdie handgedrewe mobiliteitshulpmiddel kan gesien word as ’n konvensionele handgedrewe rolstoel wat differensieel aangedryf word. Die twee grade van vryheid wat met die bewegingsplatform geassosieer word, skep geougmenteerderealiteit-navigasie in ’n denkbeeldige omgewing. Die twee grade van vryheid wat met geougmenteerderealiteit-navigasie verband hou, laat die gebruiker in ’n denkbeeldige omgewing vooruitbeweeg terwyl hapties-dinamiese terugvoer ervaar word. Die geproduseerde hapties-dinamiese terugvoer vanaf die geougmenteerde navigasie is die gevolg van gesimuleerde gravitasiekrag en traagheids-kragte soos dit in die werklikheid deur ’n gebruiker van ’n handgedrewe rolstoel ervaar sou word. Uit die bostaande is dit duidelik dat dit nodig is om behoorlike dinamiese modelle van handgedrewe rolstoele en die gebruikers daarvan op die bewegingsplatform met twee grade van vryheid te ontwikkel en te implementeer om ’n doeltreffende geougmenteerde hapties gesimuleerde omgewing te skep.

Sleutelwoorde: handgedrewe mobiliteitshulpmiddels, geougmenteerde realiteit, haptiese terugvoer, denkbeeldige omgewing

Afkortings

ADL: Aktiwiteit in daaglikse lewe
ARS: Aandrywing met reëlbare spoed
GR: Geougmenteerde realiteit
GV: Gesigsveld
GVV: Grade van vryheid
HIU: Herkonfigureerde inset-uitset
KGS: Kopgemonteerde skerm
LKR: Lineêre kwadratiese reguleerder
NI: National Instruments
PIA: Proporsionele integraalafgeleide
SP: Massamiddelpunt
VR: Virtuele realiteit

Introduction

The presented study consists of a motion simulator with a haptic interface to let the disabled individual experience the movement sensations while they navigate into a fictitious environment. Besides, they can decide on the trajectory by moving the wheelchair wheels as if they were moving across a real plane surface.

Difference method for conveying visual graphical content to the user on a virtual simulator platform are possible; the most important factor being that virtual worlds need to be conveyed to the user in near real-time. The different types of graphical interfaces may be divided into three common types: multiple screens, hemispherical displays and the use of head-mounted displays (HMD) (Steyn et al. 2014).

The designed motion platform system consists of four plasma screens to be used as a user's visual interface (Figure 1), although HMD may be used with a gyroscopic tracker (Steyn et al. 2014). Four plasma screens are used to extend the field of view (FOW) to the user's front ground view.

This paper discusses the user, the manual wheelchair and the environment interface of the motion platform. The presented platform (showed in Figure 1) is actuated by two actuators to simulate the angular movement of the user's manual wheelchair according to the user position in a fictitious environment. This fictitious environment represents the virtual architectural environment that the user will navigate. The rollers and encoders (sensors) are mounted on the motion platform in order to measure velocity feedback on both wheels of the manual wheelchair

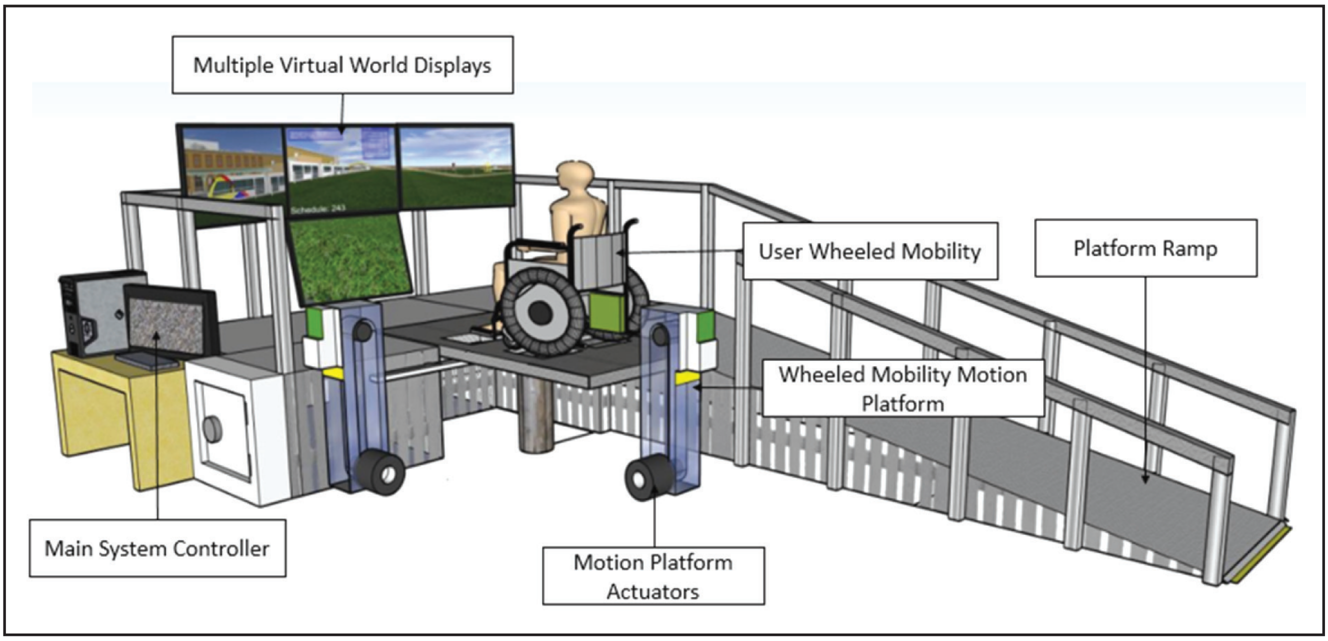

FIGURE 1: System overview interface to FOW

when the user exerts a propelling action on the wheels while interfacing with the virtual architectural environment. This implementation of the motion platform simulator will be possible by developing a control design interface that is discussed in this paper.

Differential Drive Simulator

Differential Drive of a Manual Wheelchair

The different driving wheels allow the wheelchair the ability to navigate with ease on open surfaces. If ω_L and ω_R represent the left and the right driving wheel's angular velocities, forward translation may be achieved with $\omega_L = \omega_R$ or backward translation where $-\omega_L = -\omega_R$. The rotation of the wheelchair is achieved by having $\omega_L < \omega_R$ or $\omega_L > \omega_R$. The wheelchair can rotate around the centre of the two driving wheels (c_ω) relative to the ground if $+\omega_L = -\omega_R$ or $-\omega_L = +\omega_R$ a full wheelchair rotation action. The centre point of the wheelchair determined by the centre of the two driving wheels is denoted by (c_g). A further possible wheelchair rotation occurs when the wheelchair rotates around a stationary wheel's vertical ground contact point, with one driving wheel actuated $\omega_L > 0$ and $\omega_R = 0$ or $\omega_R >$ and $\omega_L = 0$ (Steyn et al. 2014).

A representation of the wheelchair' s left and right wheel velocities, with a consequent top view wheelchair frame rotation is given in Figure 2. In the modelling of the wheelchair's dynamic responses the centre linear velocity ($V_{c\omega}$) and centre rotational velocity ($\omega_{c\omega}$) in a global reference frame are used.

The wheelchair's centre linear velocity in a global reference frame from the two differential driving wheels is given by the following equation (Steyn et al. 2014).

$$V_{c\omega} = \frac{1}{2}(V_L + V_R) \qquad 1$$

The rotation velocity ($\omega_{c\omega}$) of the wheelchair can be computed if the wheel is instantaneously moving along the arc of a circle of radius λ_s (driving shaft length):

$$\omega_{c\omega} = \frac{1}{\lambda_s}(V_L + V_R) \qquad 2$$

The wheelchair's kinematic motion, relative to its local reference frame, may then be determined as follows (Steyn et al. 2014):

$$\begin{bmatrix}\dot{x}\\ \dot{y}\\ \dot{\psi}\end{bmatrix} = \begin{bmatrix}\cos\psi & -\sin\psi & 0\\ \sin\psi & \cos\psi & 0\\ 0 & 0 & 1\end{bmatrix}\begin{bmatrix}V_{cw}\\ 0\\ \omega_{cw}\end{bmatrix} \qquad 3$$

Where $\dot{x}$ and $\dot{y}$ represent the new wheelchair velocity relative to a global reference frame and $\dot{\psi}$ represents the wheelchair's yaw or turning angle. The kinematic

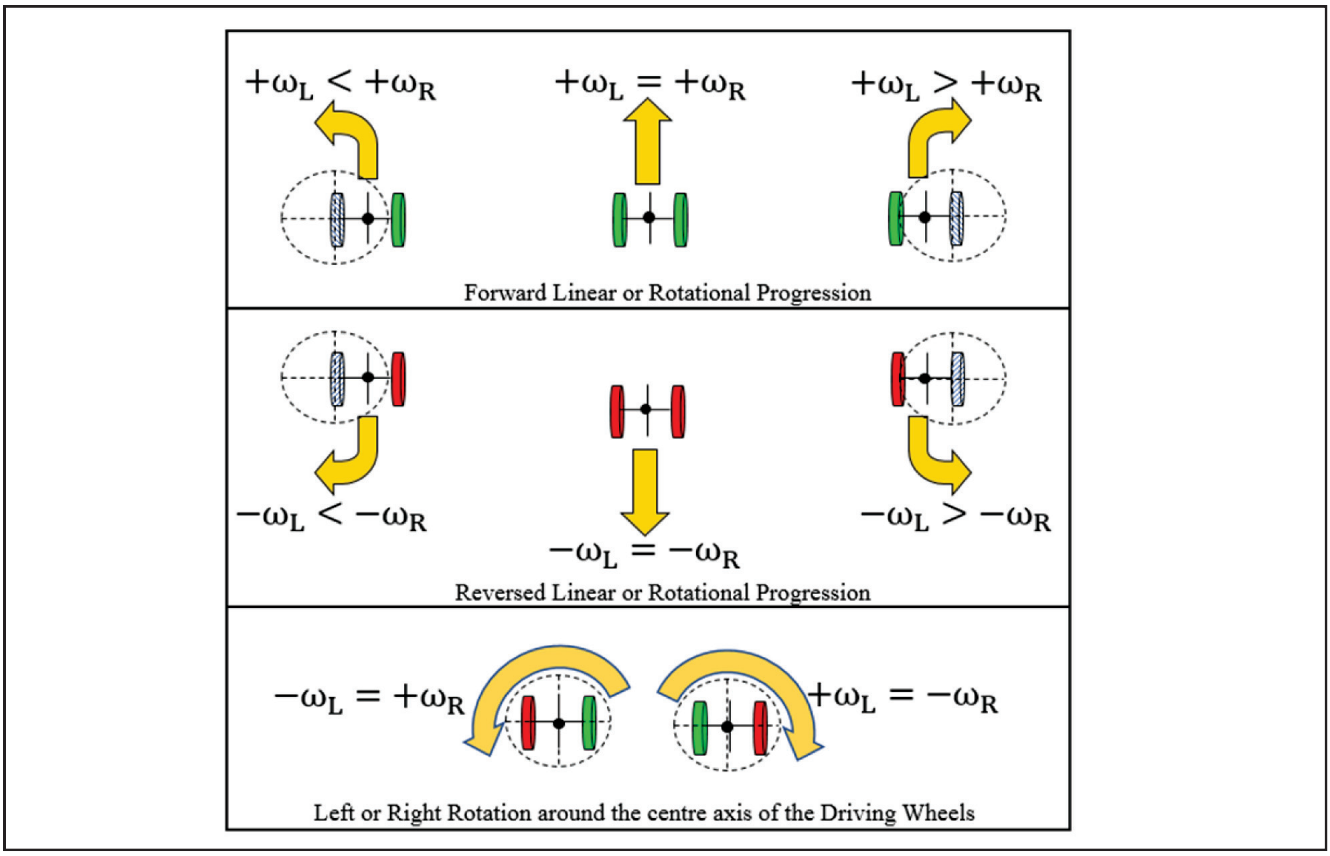

FIGURE 2: Top view representation of the differential drive configuration

model may provide information about the motion of the wheelchair, given its component differential drive wheel speed (Siegwart and Nourbakhsh 2004).

The driving action of the user causes the motion platform to encounter a velocity corresponding to wheelchair driving wheel velocities. These roller velocities are translated to the platform regulator to choose the relevant actuator's pitch or roll reactions. The motion feedback produces haptic input to the user in an augmented environment. This motion feedback is a significant element in the assessment of the user reactions to certain trajectories or to assess the performance of the user in an augmented environment in comparison to the actual environment (Steyn et al. 2014).

Based on the description of the dynamic response of a wheelchair, it is essential to define an axis system that serves as a reference for the definition of the various parameters.

Figure 3 represents a user on a manual wheelchair in an axis system and related dimensions. This is designed to represent various parameters.

A driving force related to a wheelchair consists of two independent forces, produced by the left and right wheelchair driving wheels. On a single wheel, a torque about the axis of rotation of the wheel produces a force for accelerating the wheelchair whereas a braking torque produces a force for decelerating it. To determine the dynamic equations in describing the wheel forces at ground contact, it is necessary to establish the combined wheelchair and user mass (m_{cg}) at the wheelchair's centre point of gravity. This then describes the combined masses of the wheelchair and user as a single rigid body. The wheelchair's centre linear acceleration (a_{cw}) and resultant rotational acceleration (α_{cw}) due to the produced forces is essential to define the dynamic properties. A further component, due to an inclined trajectory will be introduced to present a pitch (θ) angle of the rigid body (Steyn et al. 2014).

According to Equations 1 and 2, the wheelchair's centre linear and rotational velocity and acceleration may be calculated if the variable left (V_L) and right (V_R) wheel velocities are known:

$$a_x = ac_w = \dot{V}_{cw}$$

$$\alpha_{cw} = \dot{\omega}_{cw}$$

Equations of motion associated with the wheelchair's motion on the rollers are:

$$F_L + F_R - m_{cg}\, g \sin\theta = m_{cg} a_x \qquad 4$$

$$\frac{\lambda_s}{2} F_L - \frac{\lambda_s}{2} F_R = J_{cg}\alpha_{cw} \qquad 5$$

The resultant forces then produced at the roller or ground contact point per driving left wheel F_L and right wheel F_R may be determined from:

$$\begin{bmatrix} F_L \\ F_R \end{bmatrix} = \begin{bmatrix} \frac{1}{2} & \frac{1}{\lambda_s} \\ \frac{1}{2} & -\frac{1}{\lambda_s} \end{bmatrix} \cdot \begin{bmatrix} m_{cg}(a_x + g\sin\theta) \\ J_{cg}\alpha_{cw} \end{bmatrix}$$

Therefore,

$$\begin{bmatrix} F_L \\ F_R \end{bmatrix} = \begin{bmatrix} \frac{1}{2} m_{cg}(a_x + g\sin\theta) + \frac{1}{\lambda_s} J_{cg}\alpha_{cw} \\ \frac{1}{2} m_{cg}(a_x + g\sin\theta) - \frac{1}{\lambda_s} J_{cg}\alpha_{cw} \end{bmatrix}$$

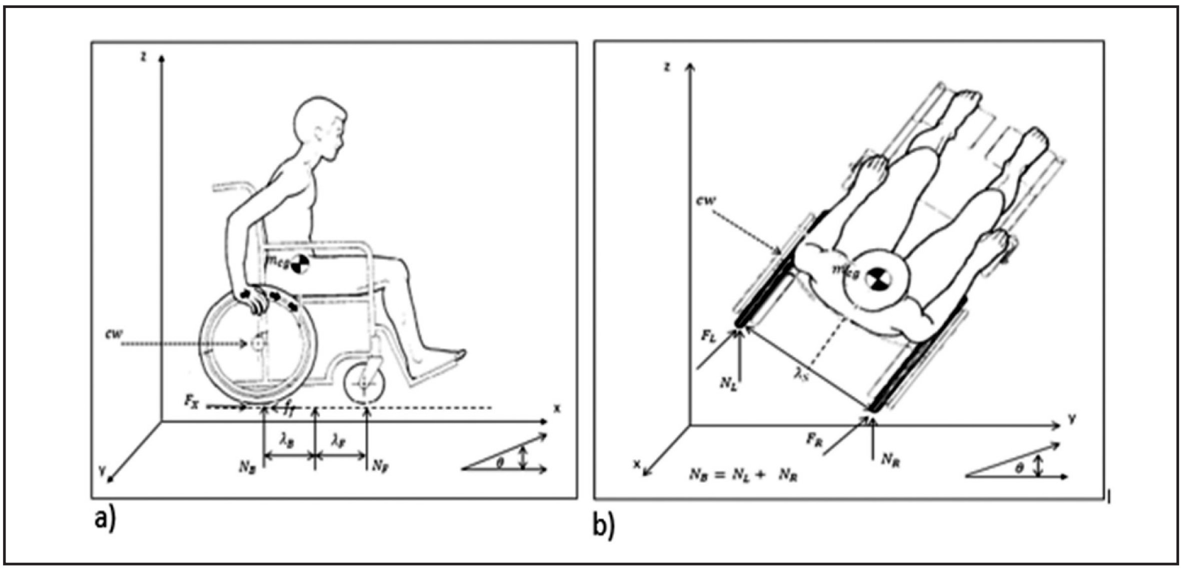

FIGURE 3: Wheelchair axis system and related dimensions: a) side view, b) top view

Where $F_R = F_{RP} - F_{RBr}$ and $F_L = F_{LP} - F_{LBr}$

F_{RP} and F_{LP} are respectively the right and the left propelling forces, while F_{RBr} and F_{LBr} are respectively the right and the left braking forces.

Wheelchair Dynamic Model

Various wheelchairs are considered as nonholonomic mechanical systems. The back wheels are independently driven by a user propelling action. The two front wheels are castor wheels. The dynamic models employed in this paper are practically identical to the proposed model in (Siegwart and Nourbakhsh 2004; Ghosal 2010). This model evaluates a third dimension which is the wheelchair on a slope and level surface.

The numerical model of the wheelchair depends on its geometry and kinematics conditions. The geometry of the wheelchair is subject to its actual development in the plane (see Figure 4) while the kinematic conditions describe its motion in place (Siegwart and Nourbakhsh 2004).

Lagrange formalism (see Equation 7) was used to derive differential equations describing the time displacement of the wheelchair yet considering the non-holonomic kinematic constraints (Siegwart and Nourbakhsh 2004).

$$\mathcal{L} = \frac{1}{2}M(\dot{x}_g + \dot{y}_g + \dot{z}_g) + \frac{1}{2}I_z\dot{\theta}^2 \; lM\dot{\theta}\cos\phi\,(\dot{x}_g\sin\theta - \dot{y}_g\cos\theta)$$
$$-Mg\sin\phi\,(\dot{x}_g\cos\theta + \dot{y}_g\sin\theta) \qquad 7$$

Considering the position of the wheelchair in the 3D space (xyz-coordinate system) indicated by $q = (x_g, y_g, z_g, \theta)^T$, with (x_g, y_g, z_g) being the Cartesian coordinate the centre of gravity of the wheelchair, and θ the angle of rotation of the wheelchair the Lagrange function is expressed in the following form:

$$M(q)\ddot{q} + C(q,\dot{q})\dot{q} + G(q) = E(q)\tau + A^T(q)\lambda \qquad 8$$

where

$$M(q) = \begin{bmatrix} M & 0 & 0 & lM\cos\phi\sin\theta \\ 0 & M & 0 & -lM\cos\phi\cos\theta \\ 0 & 0 & M & 0 \\ lM\cos\phi\sin\theta & -lM\cos\phi\cos\theta & 0 & I_z \end{bmatrix}$$

$$C(q,\dot{q}) = \begin{bmatrix} 0 & 0 & 0 & \dot{\theta}lM\cos\phi\cos\theta \\ 0 & 0 & 0 & \dot{\theta}lM\cos\phi\sin\theta \\ 0 & 0 & 0 & 0 \\ 0 & 0 & 0 & 0 \end{bmatrix}$$

$$G(q) = \begin{bmatrix} Mg\sin\phi\cos\theta \\ Mg\sin\phi\sin\theta \\ 0 \\ Mg\sin\phi\,(y_g\cos\theta - x_g\sin\theta) \end{bmatrix}$$

$$E(q)_{4\times 2} = \begin{bmatrix} \frac{\cos\theta}{r} & \frac{\cos\theta}{r} \\ \frac{\sin\theta}{r} & \frac{\sin\theta}{r} \\ 0 & 0 \\ \frac{b}{r} & \frac{-b}{r} \end{bmatrix}, \tau = \begin{bmatrix} \tau_R \\ \tau_L \end{bmatrix}$$

$$A(q)_{2\times 4} = \begin{bmatrix} -\cos\phi\sin\theta & \cos\phi\cos\theta & \sin\phi & -l \\ \sin\phi\sin\theta & -\sin\phi\cos\theta & \cos\phi & 0 \end{bmatrix}$$

λ is the vector of Lagrange multipliers. The left and right torque are designated by T_L and T_R respectively. When both are equal, a rectilinear motion occurs and rotational motion in the contrary case.

In the case of the wheelchair wheels roll without slipping, lateral motions are not plausible; subsequently the network related with the nonholonomic constraints is perpendicular to the pivot of the driving wheels written in condition form as $A=(q)\,\dot{q}= 0$ (Siegwart and Nourbakhsh 2004):

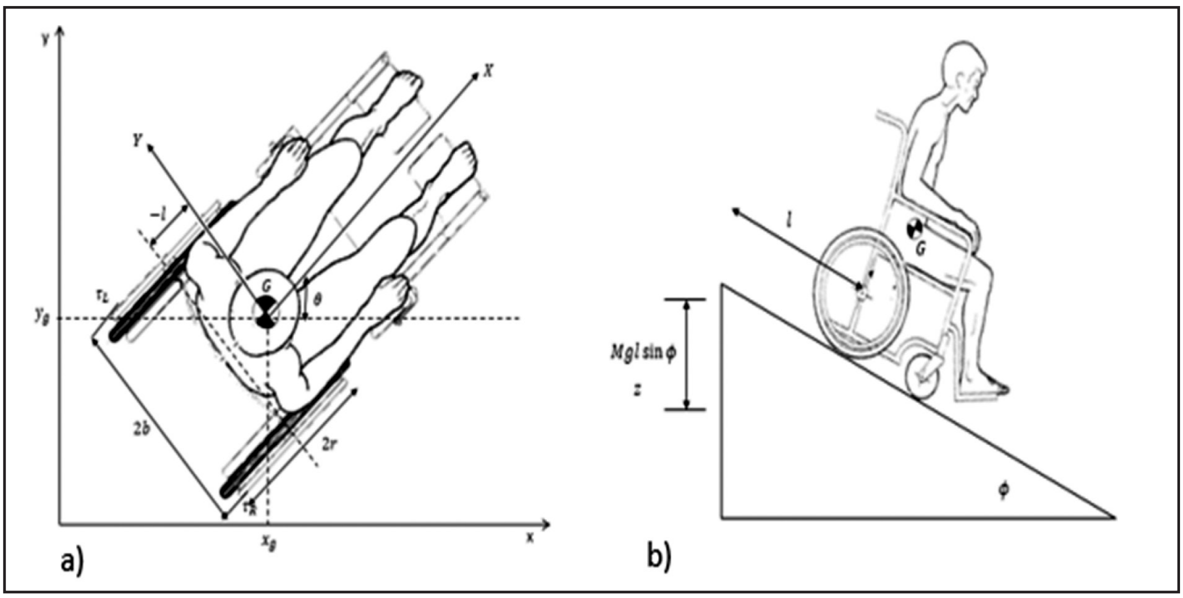

FIGURE 4: Manual wheelchair a) on a flat plane. b) on an incline plane

Considering $S(q) \in \mathbb{R}^{n\times m}$, a set of smooth and linearly independent vector fields spanning the null space of $A(q)$ such that $S^T(q)\,A^T(q) = 0$, we derive the kinetic equation as follows:

$$\dot{q} = S(q)\eta \qquad 9$$

With

$$S(q) = \begin{bmatrix} \cos\theta & -l\cos\phi\sin\theta \\ \sin\theta & l\cos\phi\cos\phi \\ 0 & l\sin\phi \\ 0 & 1 \end{bmatrix} \text{ and } \eta = \begin{bmatrix} \upsilon \\ \omega \end{bmatrix}$$

The velocities υ and ω are respectively the linear and angular velocities of the distinguished point G, the centre of gravity of the wheelchair and user combined.

The derivative of Equation 8 with respect to time gives:

$$\ddot{q} = \dot{S}(q)\eta + S(q)\dot{\eta} \qquad 10$$

with the matrix:

$$\dot{S}(q) = \begin{bmatrix} -\dot{\theta}\sin\theta & -\dot{\theta}l\cos\phi\cos\theta \\ \dot{\theta}\cos\theta & -\dot{\theta}l\cos\phi\sin\theta \\ 0 & 0 \\ 0 & 0 \end{bmatrix}$$

By taking Equations 9 and 10 into Equation 8 and after simplification, we obtain a more appropriate control system representation for the dynamic model of the wheelchair as follows:

$$\begin{bmatrix} \dot{\upsilon} \\ \dot{\omega} \end{bmatrix} = \begin{bmatrix} -g\sin\theta \\ \dfrac{Mg\sin\phi\,(y_g\cos\theta - x_g\sin\theta)}{Ml^2\cos 2\phi - I_z} \end{bmatrix} + \begin{bmatrix} \dfrac{1}{Mr} & \dfrac{1}{Mr} \\ \dfrac{b}{r(I_z - Ml^2\cos 2\phi)} & \dfrac{b}{r(I_z - Ml^2\cos 2\phi)} \end{bmatrix} \begin{bmatrix} \tau_R \\ \tau_L \end{bmatrix}$$

System Integration and Hardware Design

The presented system is designed around two controllers running on windows-based platforms that rely on the fact that independent development is able to be carried out in parallel, and the virtual world (fictitious environment interface with the user) may be used as a separate unit. The integration into a single system controller is possible and may be a consideration for developing the next generation of a virtual reality motion platform in an enabling environment. The interconnection between all the different subsystems associated with the motion platform, the wheelchair and the user are depicted in Figure 5. The system clearly consists of subsystems interconnected to form a complete motion platform with sensors, a controller and actuators to produce visual and physical feedback to a user. The user action, due to trajectory planning, generates the desired system set-point (SP) that determines the level of intensity of motion feedback of the motion platform.

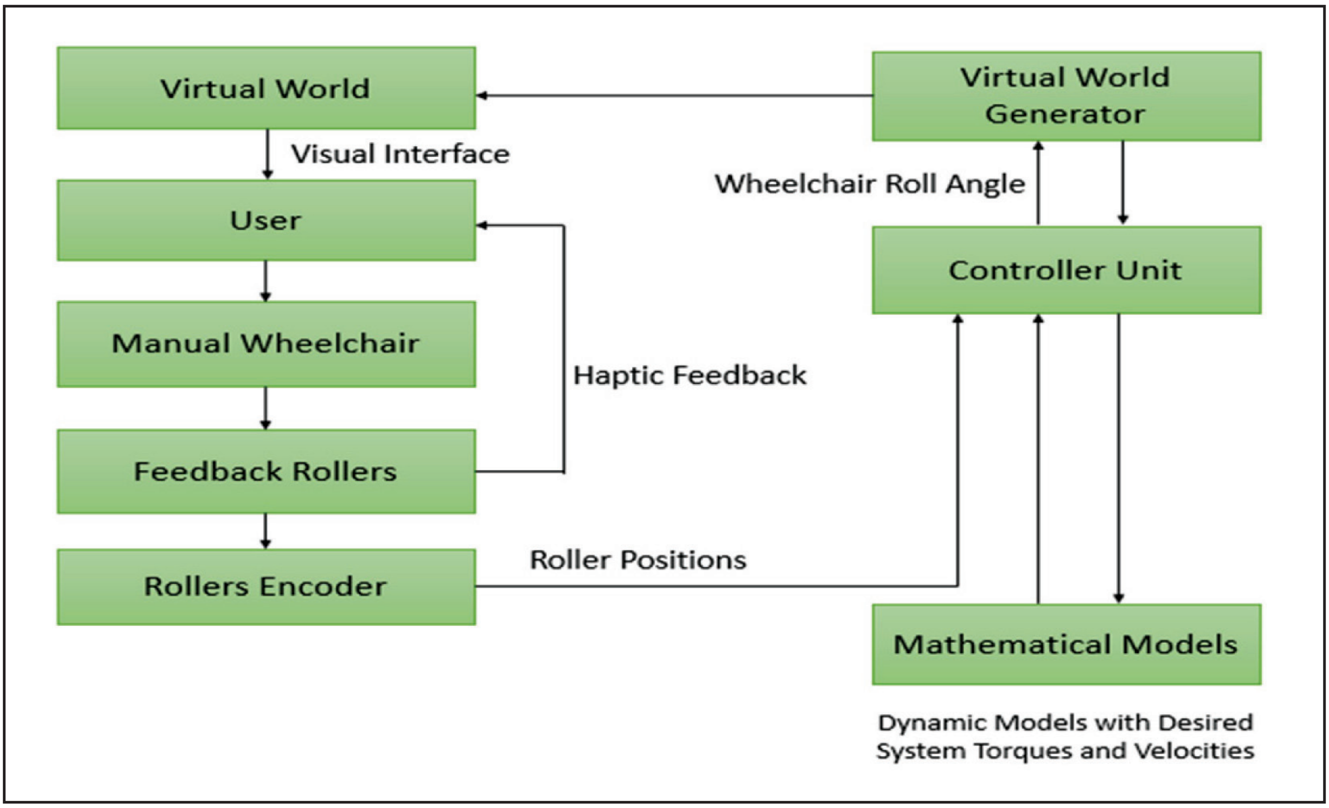

FIGURE 5: Subsystem interconnection block diagram

This motion feedback in the two degrees of freedom (2-DOF) relies on the type of trajectories encountered by the user in the virtual world. The user action with wheelchair velocity and turning ratio determine the velocities of experienced actuator motion in the two degrees of freedom (2-DOF) motion. Finally, the feedback motions controlled by the system consequently consist of platform pitch and roll actions with the wheelchair wheel roller resistance to simulate dynamic wheelchair properties in the form of torque control.

System Actuator Design

The different sensors used in the design and their purpose consist mainly of determining wheelchair and system positions, velocities and accelerations (Steyn et al. 2014). The types of sensors used for the latter are three-channel digital pulse generating rotary encoders. These are installed on all the feedback variables necessary for control as in the actuator motion and the wheelchair motion.

The position encoders used for the wheelchair's independent driven wheel velocities are used to map the intended path to be produced in the virtual world. The wheelchair's two driving wheels are placed in direct contact with rollers to measure the differential driving motion with the rotary encoders mounted on each roller pair depicted in Figure 6. If ω_L and $\omega_g$represent the left and right angular velocities of the wheelchair's driving wheels respectively, forward and backward translations are computed using ω_L and ω_R. The rotation of the wheelchair is achieved by having $\omega_L < \omega_g$ or $\omega_L > \omega_g$.

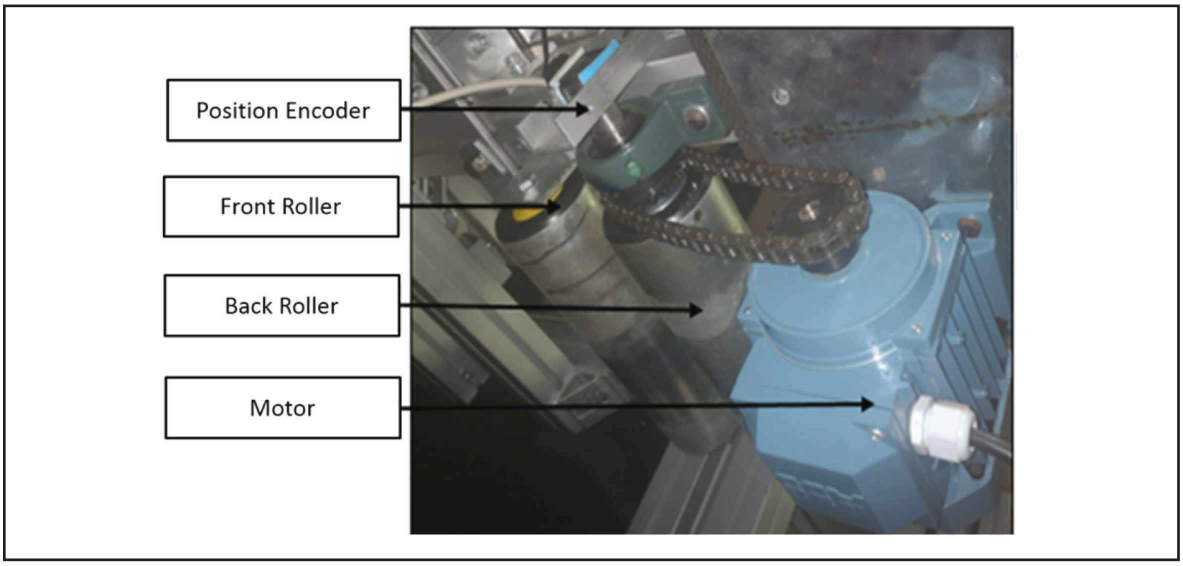

FIGURE 6: Position encoder mounted on a roller pair

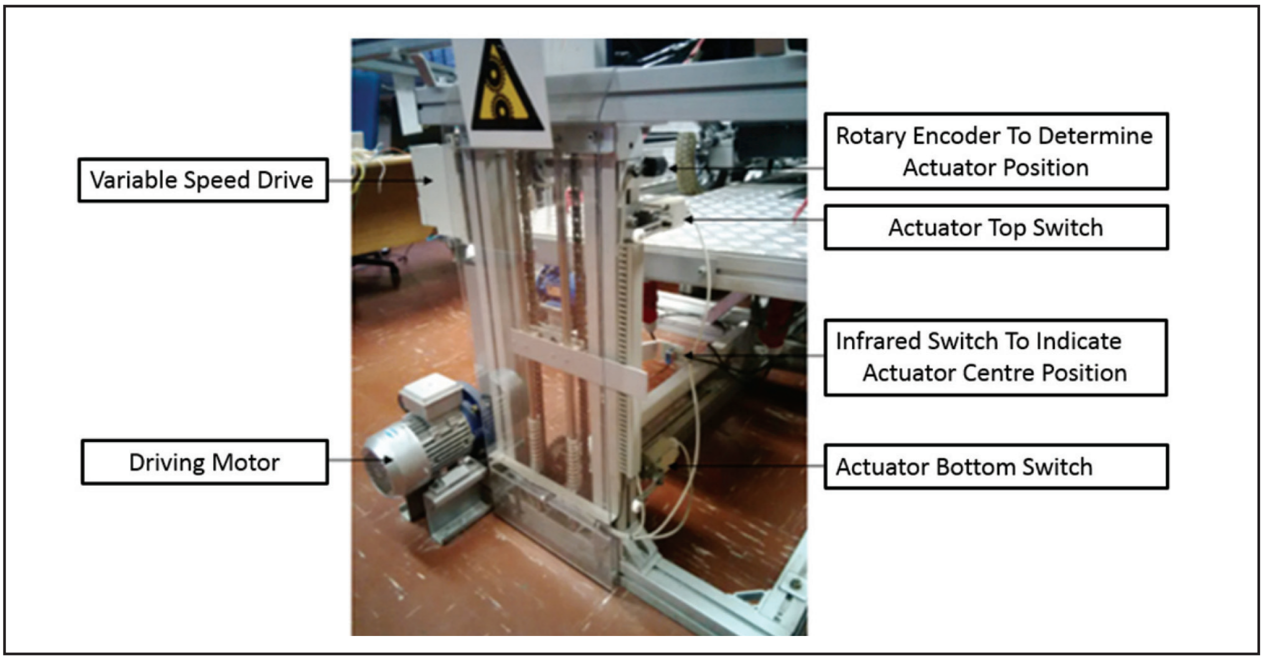

FIGURE 7: Single prismatic actuator's main mechanical and electrical components

The position encoders on the prismatic actuators determine the linear positions of actuator displacement so as to achieve a desired controlled position, in order to simulate the motion platform's pitch and roll actions. The different pitch and roll actuator sensors for a single motion prismatic actuator may be view in Figure 7. Limit switches are used to measure critical actuator limit and zero positions. These switches are placed on the actuators' linear translations to determine the end of travel. This mechanical limit switch protects the actuator against possible overshoot which might cause damage to the mechanical system. Infrared reflective sensors are used to determine zero-degree positions (centred) on both the linear actuators. Zero position sensing is used to reset actuator positions so as to eliminate any drift due to mechanical slippage or electrical signal errors.

System Control Design and Discussion

A Linear Quadratic Regulator (LQR) has been designed to simulate the pitch and roll platform dynamics which is connected to the real-time fictitious environment.

TABLE 1: Variables

Variables	Units	Description
$\ddot{x}$	m/s^2	Longitudinal acceleration
$\ddot{y}$	m/s^2	Lateral acceleration
θ	degrees	Roll angle
ϕ	degrees	Pitch angle
u	V	Command for θ_d and ϕ_d
$M_{1,2,3}$	–	Electric motor 1, 2, 3

The control design strategy based on the LQR structure is presented in this section. The objective of the control design is to obtain a linear transfer matrix that minimises a quadratic cost function involving the tracking error and the motion platform simulator output (actuators) by considering the physical constraint of the motion platform. The proposed controlled output for tracking is given by:

$$y = [\ddot{x}\ \ \ddot{y}\ \ \theta\ \phi]^T \qquad 11$$

Where all variables are measured from the motion platform simulator. Such that the control tracking error is given by:

$$e \equiv y_m - y \qquad 12$$

where y_m is a vector that constraints the motion platform variables corresponding to the measured ones. These variables are described in Table 1.

To ensure the motion platform simulator constraints and the minimisation of the tracking error between the simulated manual wheelchair and the experimental motion platform, the equation to design an optimal control based LQR is given by:

$$J = \int_{t_1}^{t_2} (e^T Qe + u^T Ru)dt \qquad 13$$

where u is the controller output that manipulates the three electric motors, $[t_1, t_2]$ is the residence time horizon of the motion platform simulator, while Q and R are the weighting matrices given by the proposed LQR based motion platform is schematised in Figure 8.

Interface Design

User Haptic Feedback

The inertial feedback system simulates gravitational forces. It refers to the linear and rotational inertia a user will experience on both the left and right driving wheels in a real environment when driving a wheelchair, that will represent the user haptic feedback. This force haptic feedback is exerted on the roller system of the motion platform hosting the wheelchair's two differential driving wheels. The aim of the force haptic feedback is to generate the linear and rotational inertia on the manual wheelchair user while navigating in a fictitious environment. Independent opposite force feedback is produced on each roller by a user's propelling action determined by the driving forces F_L and F_R as in Equation 6.

In Figure 9, the representation of a single roller feedback system may be observed with the wheelchair's driving wheel at a velocity $+\omega_w$ and in direct contact with the actuated force feedback roller (rx). F_x represents a single friction force related to either F_L or F_R. The variables ω_m and τ_m represent the motorised actuator's velocity and produced torque.

The actuator and roller are linked via a chain to an electric motorised actuator. The total chain tension may be represented by $T_c = T_{c1} + T_{c2}$. Only the total tension T_c of the upper and lower chains will be considered, since the actual tension will include the pretensions which are not determined in this system.

From the friction forces of Equation 5, generated by the left and right wheels of the wheelchair's differential driving system, the following equations of the angular momentum may be derived associated with the rollers and feedback motors:

$$M_m - T_c r_m = J_m \alpha_m \qquad 14$$

$$T_c r_r = J_r \alpha_r \qquad 15$$

where the chain tension $T_c = F_L$ or F_R and M_m are the left or right motors' desired moment.

A constraint on the motion is that the linear acceleration of the chain and the two sprocket contact points must be equal:

$$\alpha_r r_r = \alpha_m r_m \qquad 16$$

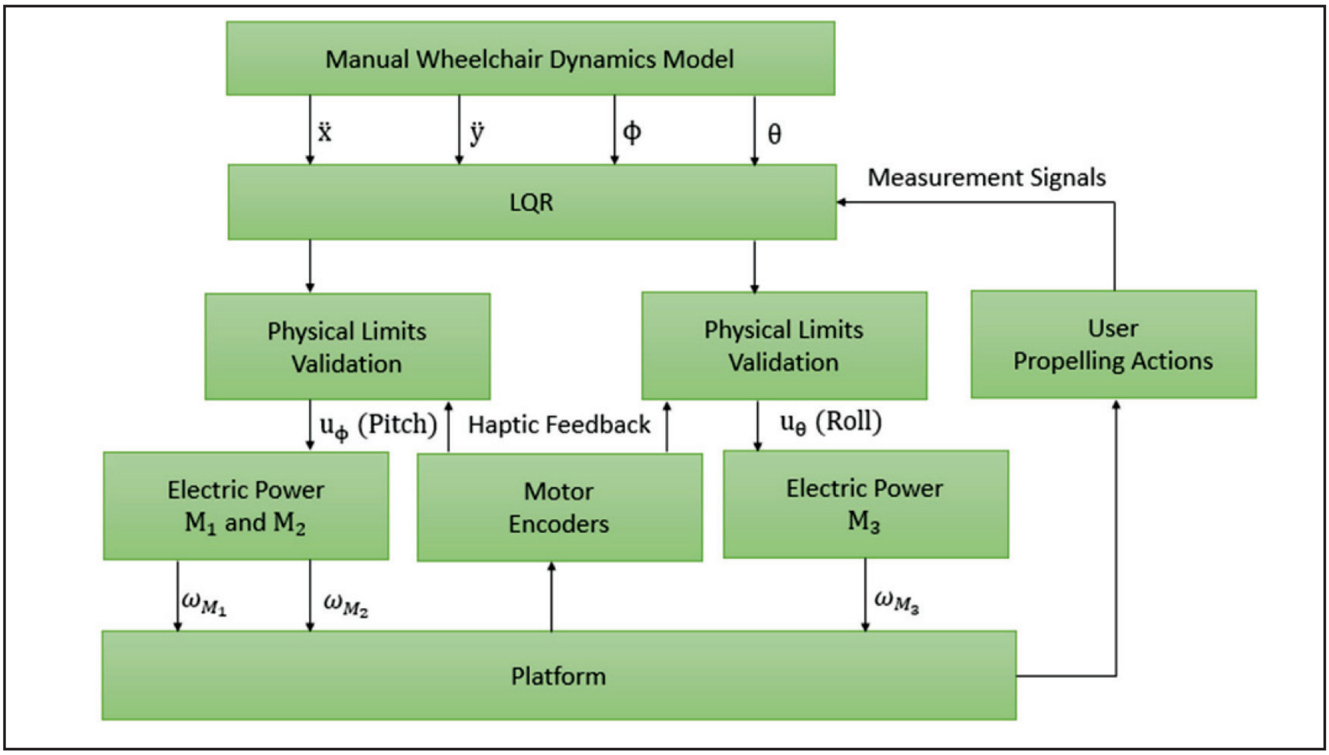

FIGURE 8: Block diagram of the LQR based motion platform

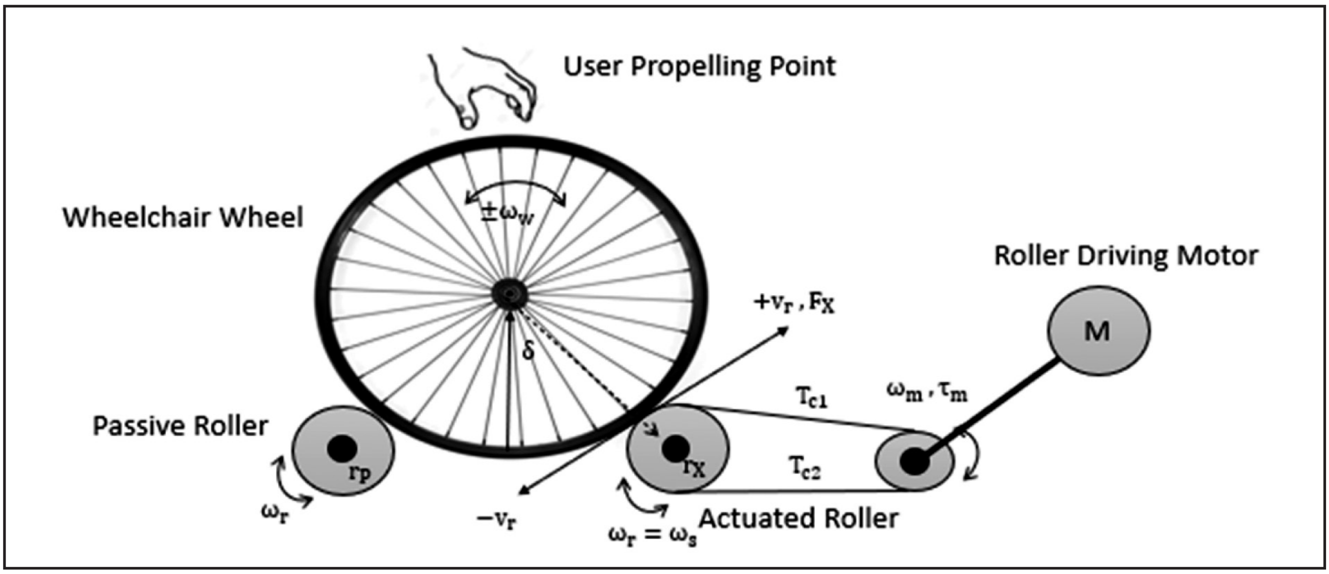

FIGURE 9: A single driving wheel's roller force feedback system representation

By substituting Equation 16 into Equation 14 in terms of α_m and again Equation 15 into Equation 14 in terms of α_r, the desired torque needed by the left (M_{mL}) and right (M_{mR}) motors to generate feedback on the rollers to simulate wheelchair inertial forces and gravity forces becomes:

$$M_{mL} = F_L\left(r_m + \frac{J_m r_r^2}{J_r r_m}\right) \quad 17$$

$$M_{mR} = F_R\left(r_m + \frac{J_m r_r^2}{J_r r_m}\right) \quad 18$$

With J_r the roller inertia, and J_m the electric motor inertia, for both the left and right feedback motors. The link between the motor and chain is achieved by a sprocket with a diameter r_m while a roller's diameter is equal to r_r.

Visual Interface

The visual interface with the manual wheelchair user is constituted by a moving platform of four degrees of freedom and a haptic system. The platform allows the user to transmit the accelerations to which he/she is subjected as an effect of the navigation that takes place in the fictitious environment. It also allows reproducing the different inclinations of the terrain of the virtual world on which the user is moving. Regarding the haptic system, it consists of two active rollers driven by motors that serve as the interface with the manual wheelchair, which must be positioned so that the wheels are in permanent contact with the rollers. They have two functions. On the one hand, the rollers are activated when the user moves the manual wheelchair's wheels and detect the intention of the user's propelling action. On the other hand, they emulate the conditions of the surface of the fictitious environment with the movement of the rollers. That is, depending on the inclination and surface of the fictitious environment in which the user is located, the user may even notice ease when moving the wheels. The motion platform and the active rollers mounted can be observed in Figure 10. The motion platform control unit is responsible for measuring and processing the movement of the rollers, as well as generating the rotation to the rollers that corresponds to the one experienced by the wheels of the virtual wheelchair. The communication between the user's manual wheelchair on the motion platform and the virtual world is performed by using the Labjack device.

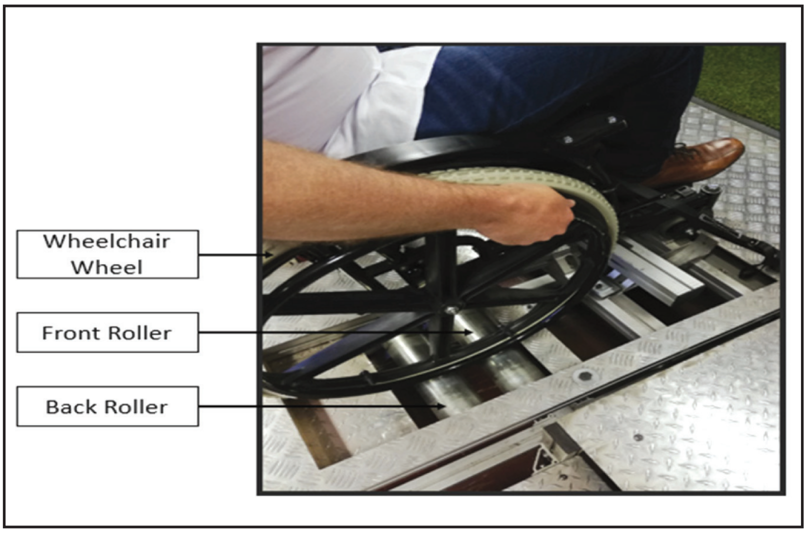

FIGURE 10: Motion platform roller top view

Results

In the preceding section, the design of the differential drive of a manual wheelchair and the controller design were presented to integrate the user, the manual wheelchair, and the environment interface to the motion platform. The focus of this section is to analyse the implemented results of the user by propelling himself on a manual wheelchair. To obtain a clear idea of this results, the system control design block diagram (see Figure 11) and the user navigation representation (see Figure 12) is depicted.

Figure 11 depicts the control design block diagram. In this figure, the encoder signal, user input velocity, actuated roller velocity, controller unit, roller actuator and roller encoder are presented. During the user propelling action, a roller velocity is produced and measured by the encoder. The produced roller velocity (encoder signal) is further measured by the system input to determine its degree of steepness (gradient). If the produced roller velocity gradient is positive, the system SP (setpoint) is the user velocity input (roller velocity produced by user propelling action). And if the produced roller velocity is negative, the system SP will be the actuated roller velocity. The actuated roller velocity is produced by the dynamic of the manual wheelchair user represented in Equation 6. This dynamic depends on the user propelling action in order to actuate the roller. The system SP (user input velocity or actuated roller velocity) is compared to the actual roller velocity (measured by the system encoder), and the resulting error signal is introduced to the controller unit. The controller unit produced a control signal that will be used to drive the roller actuator to the desired setpoint. The desired setpoint is the user input velocity and the actuated roller velocity. The presented control design may be applied on the left and right rollers attached to the manual wheelchair wheels to produce a

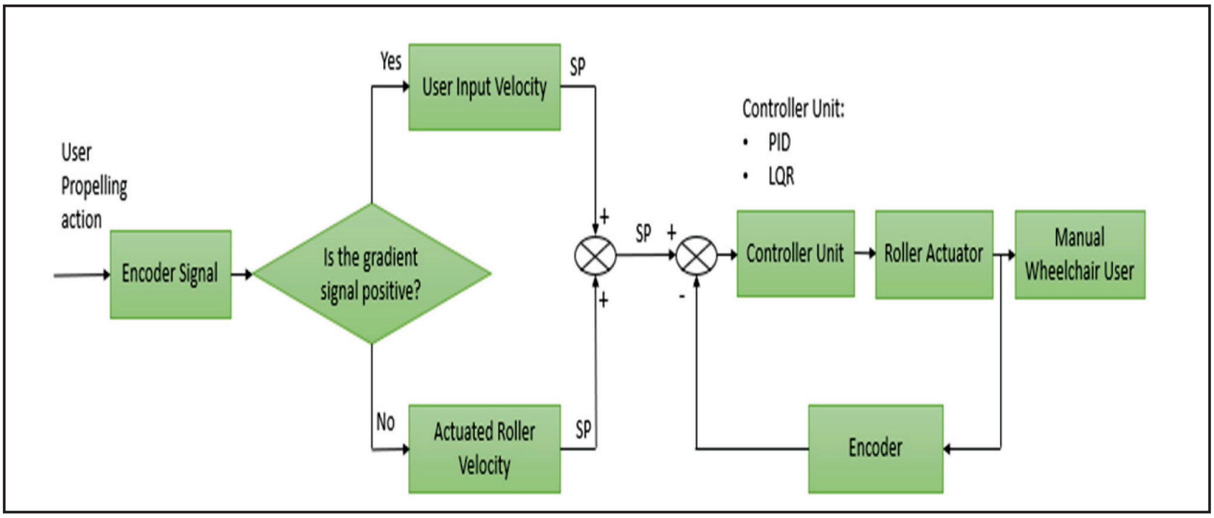

FIGURE 11: Control Design Block Diagram

differential drive. This differential drive will then produce to the manual wheelchair user a dynamic feeling as would be experienced in a real environment.

Figure 12 depicts the user differential drive representation in the fictitious environment. In this representation, the main components are encoder input signal, controller, system encoders and user navigation in the virtual world. During the user propelling action, the encoder reads the user input signal (user propelling action). The user input signal is then compared with the system encoder signals (rollers actuator measurement); the resulting signal (error signal) is then processed to the system controller. The system controller produces a controlled signal that will be integrated into the system roller actuators to drive the system rollers, the system roller signal is then translated to the user navigation in the fictitious environment. The user navigation of the manual wheelchair may be presented as a linear motion into the fictitious environment. The linear progression into the virtual world is employed for the user to experience a realistic feeling of navigation on the manual wheelchair. The implemented results of these motion will be presented in this section using the LQR and PID controller.

User Input Propulsion

The results presented in this section are the measured user input velocity while propelling on the manual wheelchair wheels, mounted on the system rollers and encoders. The system encoders are responsible for measuring the user velocity on the manual wheelchair. The produced user velocity may be used as a predicted manual wheelchair user velocity to implement a realistic dynamic signal to be sent to the system actuators to drive the system rollers, which will contribute to the manual wheelchair user experiencing the navigation in a fictitious environment while propelling the manual wheelchair wheels.

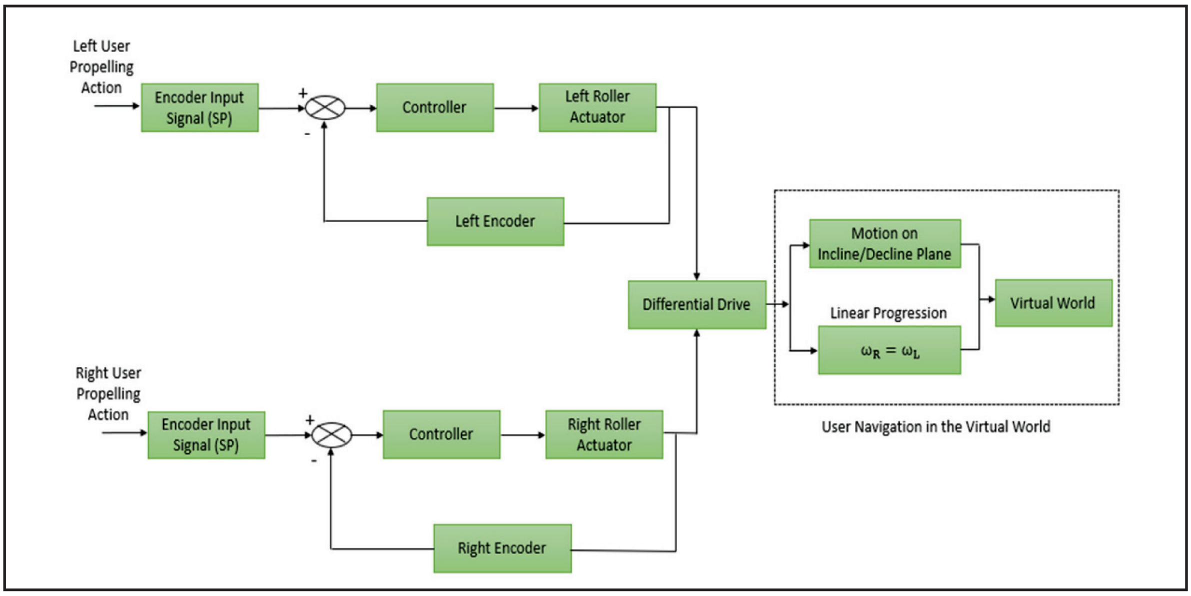

FIGURE 12: User navigation representation

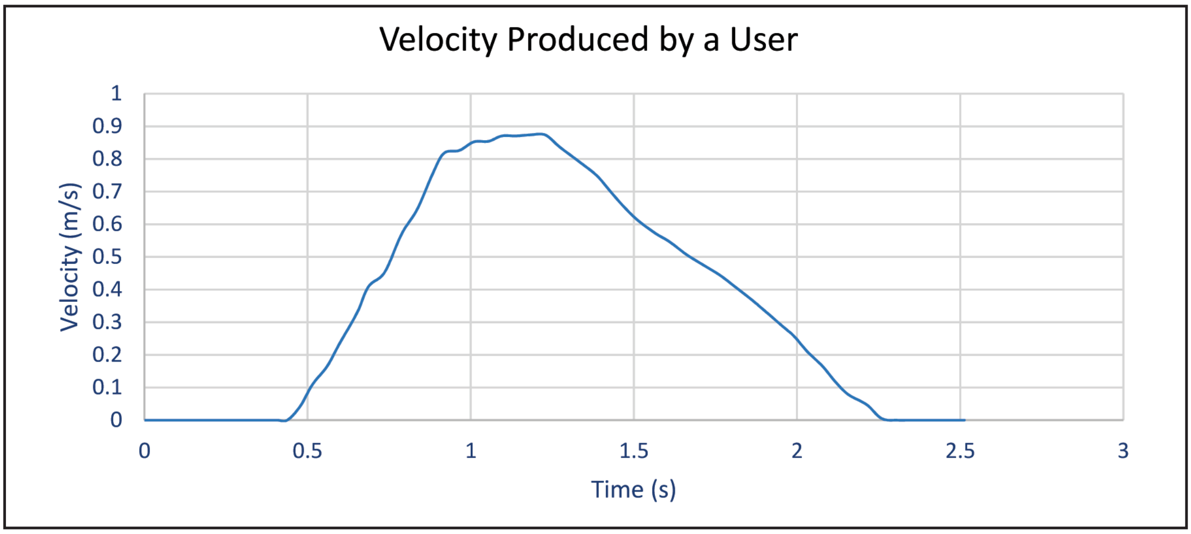

FIGURE 13: User propelling action signal

Figure 13 presents the results of the produced user input velocity while exerting a propelling action on the manual wheelchair wheels mounted on the system rollers. This figure presents the measured velocity (0.9 m/s) of the system encoders produced by the user applying a propelling action force on the manual wheelchair wheels.

Figure 14 represents the roller velocity and the variable speed drive (VSD) signal. The presented roller velocity is a single propelling action produced by the user. This result may be divided into two parts, the user input (produced velocity) and the required VSD signal. The required VSD signal is used to drive the system roller to produce a dynamic feeling to be experienced in a real environment. This dynamic feeling may be experienced on the left and right rollers.

Figure 15 illustrates a manual wheelchair user propelling action; this figure depicts the result obtained in Figure 14. As shown in Figure 14, the roller velocity (user input velocity) gradient becomes negative after the user exerts a propelling action, then the roller is actuated in order to mimic a dynamic feeling as experience in a real environment.

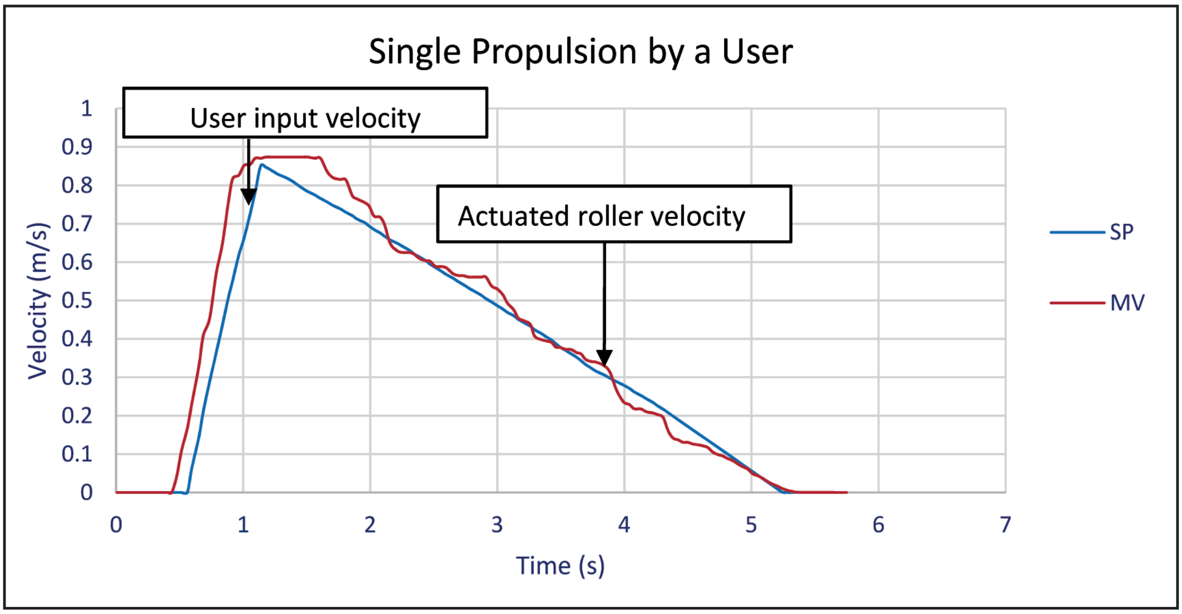

FIGURE 14: Implemented single speed ramp response

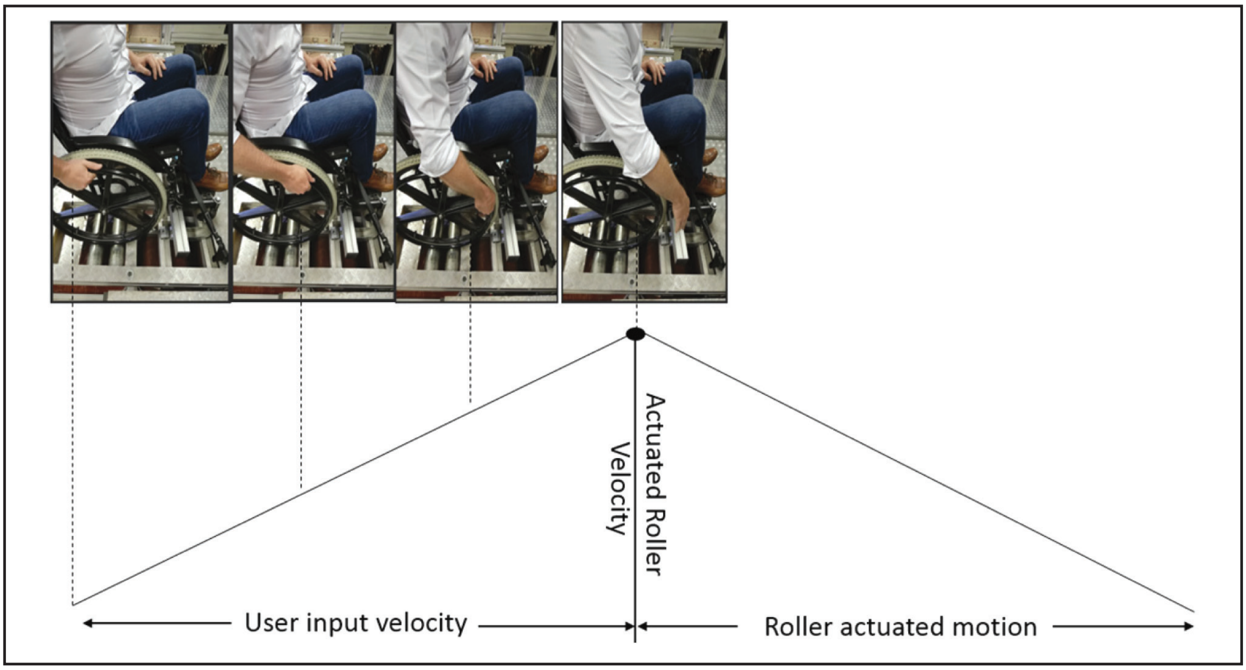

FIGURE 15: Illustration of a manual wheelchair user propelling action

System Implemented Results

In this section, the ramp signal may be presented as a user propelling action (user velocity input) on a manual wheelchair mounted on the system roller encoders. The signals of the system roller encoders are presented in section 4.1. During the user navigation (user propelling action), the roller actuator signals are measured by the system encoder, and the signal differences (error signal) between the user propelling action and the measured roller actuator is introduced to the system controller. The error signal is then processed by the system controller that produced a controlled signal (manipulated variable). The actual manipulated variable (MV) in the subsequent figures in this section represent the actual results by implementing the PID and LQR design.

PID Step and Ramp Response

Figure 16 presents the actual results of the system step response of the PID controller. In this figure the step signals (0.5m/s, 0.7ms and 1m/s) are used to investigate the system behaviour (system response) by using the PID controller. According to the results obtained in Figure 16, the system manipulated variable (MV) follows the system setpoint (SP) successfully.

Figure 17 shows the actual results of the system user propelling action (user velocity input) response of the PID controller. The user propelling action is exerted on the manual wheelchair wheels that are mounted on the system roller encoders, thus producing a velocity on the system rollers as discussed in section 4.1. The system

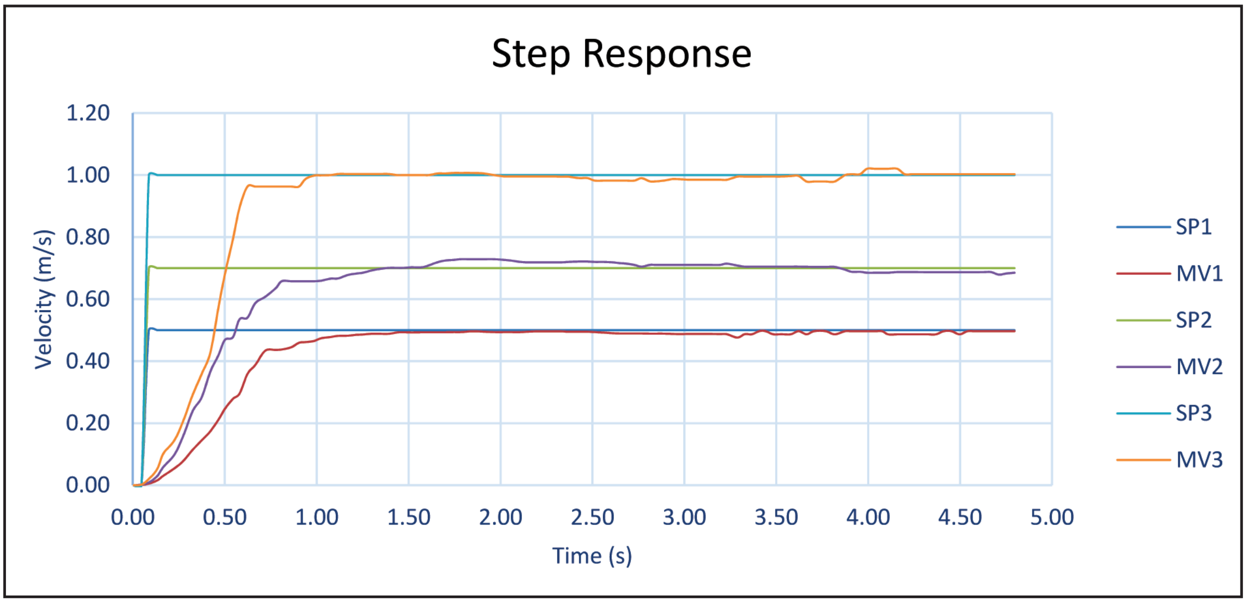

FIGURE 16: Implemented speed step response of the PID controller

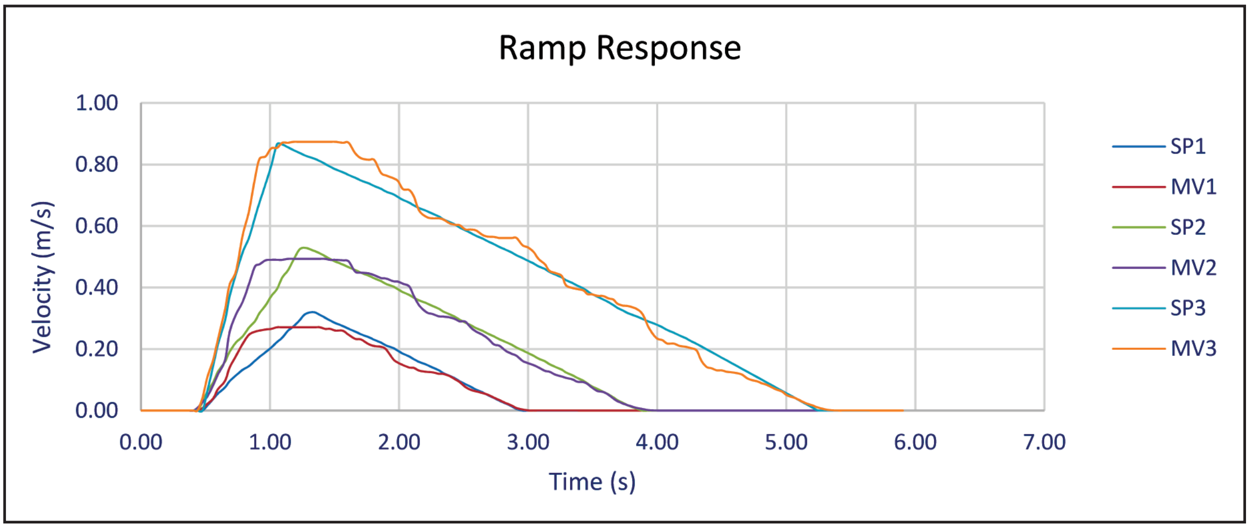

FIGURE 17: Implemented speed ramp response of the PID controller

rollers velocity is the actual user input and is presented as a set-point (SP), the controller will then use this set-point to produce a controlled signal (MV) that tracks the user input (ramp input) as displayed in Figure 17. In this result, three user velocity input responses were implemented.

LQR Step and Ramp Response

Figure 18 represents the actual results of the system step response of the LQR controller. This figure depicts the velocity signals (0.5m/s, 0.7ms and 1m/s) generated by a step input to determine the system response using LQR controller. As shown in Figure 18, the system was successfully responding to the step input.

Figure 19 depicts the user propelling action (generated user velocities) response using the LQR controller. In the next figure, the result of the performance between the LQR and PID will be depicted.

Figure 20 presents the system performance of the LQR and PID controller by measuring the torque of the system rollers while the user exerts a propelling action on the wheelchair wheels. This figure clearly shows that the LQR controller presents a better performance compare to the PID controller.
The results presented in Figures 17 and 19 represent the controlled signal that is integrated into the system roller

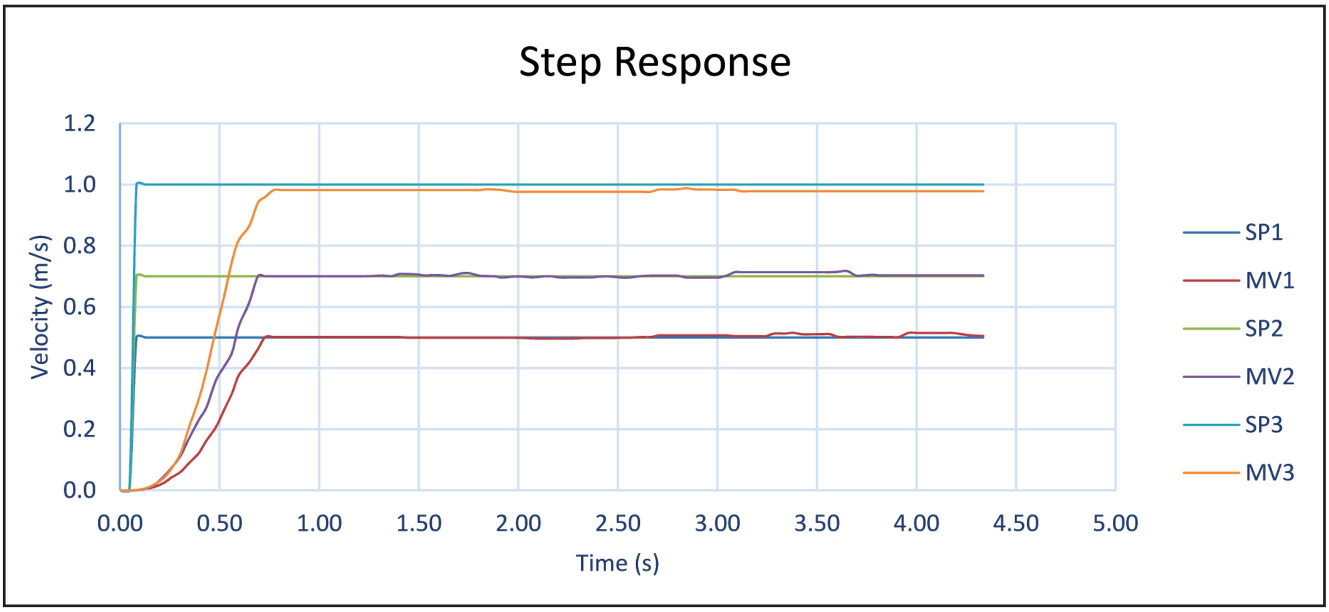

FIGURE 18: Implemented speed step response of the LQR controller

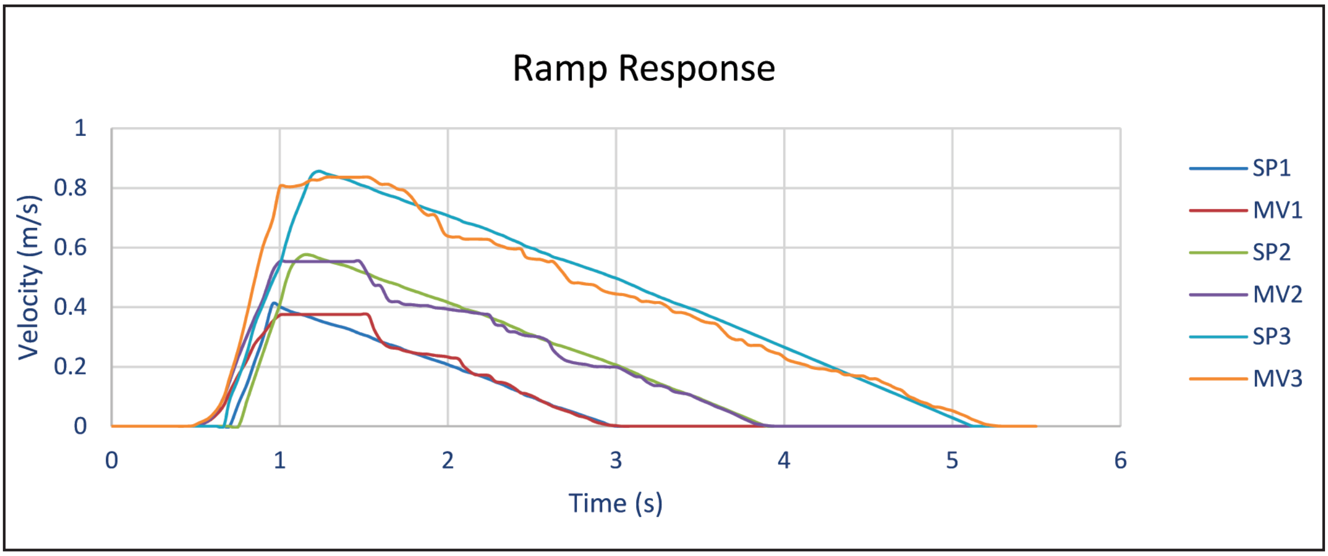

FIGURE 19: Implemented speed ramp response of the LQR controller

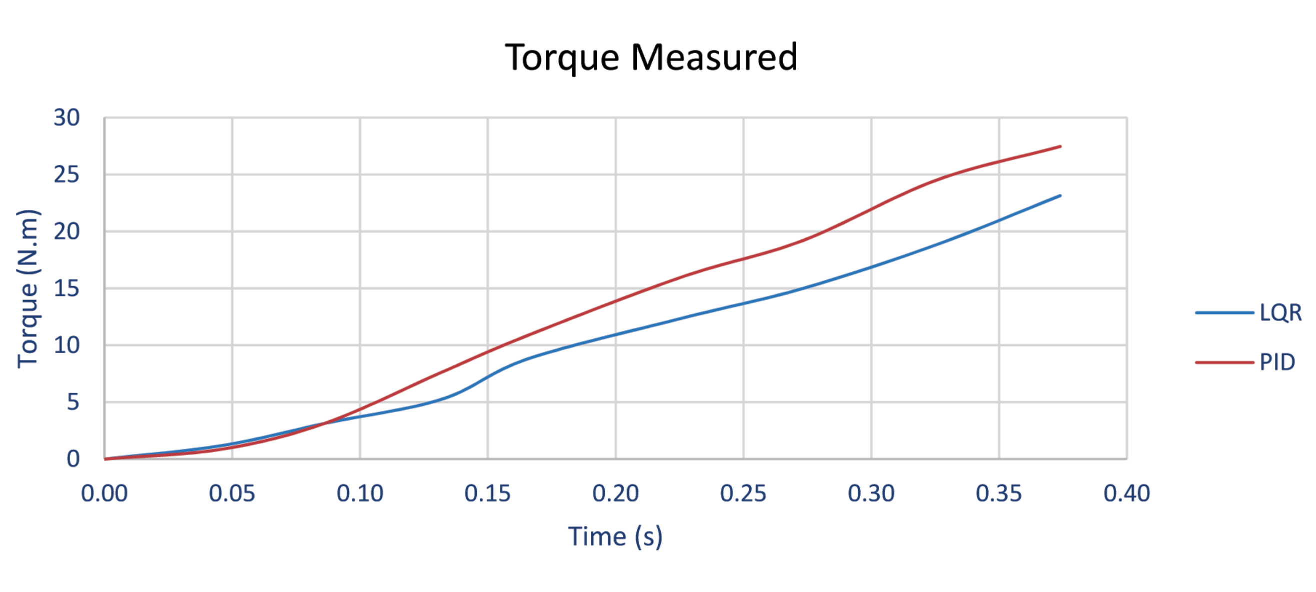

FIGURE 20: System performance of the LQR and PID controller

actuators to determine the user motion of the manual wheelchair (linear progression and the motion on an incline and decline) by actuating the system rollers. The roller actuation is then translated to the virtual environment for the user to experience realistic navigation while seated on the manual wheelchair.

Conclusion

In this paper, the main objective was to develop the dynamic model of haptic feedback on a manual wheelchair for the two degrees of freedom (2-DOF) motion platform used in an augmented reality environment for manual wheelchair driving. This serves as a motivation to help to train disabled people to drive wheelchairs.

The other part of this paper was to model and control the roller for the feedback of the manual wheelchair wheels during the user propelling action.

The dynamic model of the two degrees of freedom (2-DOF) motion platform and the haptic feedback are the major contributions of this work.

The controller for the roller was also developed. The controller is based on PID and LQR. The implemented results demonstrated that the LQR results were stable.

Acknowledgements

First and foremost, my sincere gratitude and appreciation go to my supervisors: Dr Nico Steyn and Prof Karim Djouani for their patience, all guidance and support they have given me. I thank Prof Anish Kurien for all the administrative support. I would like to particularly thank Dr Nico Steyn for support, patience and guidance; he has been a great source of motivation to continue with my studies.

Sources of funding

I would like to thank the Tshwane University of Technology (TUT), the French South African Institute of Technology (F'SATI) and the National Research Foundation (NRF) for providing financial support and research materials that enabled the smooth running of this work (NRF Grant Number: 90604).

Contribution of each author

Nico Steyn conceived the presented research project idea. Franck Boukila developed the research theory and performed the computations. Nico Steyn and Karim Djouani verified the research analytic methods and supervised the findings of this journal paper.

References

Alma, S.M., David, J. 2002. Virtual real-augmented rehabilitation for patient following stock, International Conference on Disability, Virtual Reality and Associated Technologies (ICDVRAT), ESBJEG. 82(1), pp. 898-915. https://doi.org/10.1093/ptj/82.9.898.

Anna, D. 2017. https://teslasuit.io/blog/haptic_feedback/ [Accessed 02 July 2018].

Apoora, B., Anunary, R. 2016. Human Computer Interface-Augmented Reality, International Journal of Engineering Science and Computing, 6 (1), pp. 2595-2595.

Calle, T., Ueda, J., Springle, S., Ferri, A. 2014. Development of a Control System to Determine Influence of Rolling Resistance in Manual Wheelchair Dynamics and Mechanical Efficiency Georgia Institute of Technology, Journal of Rehabilitation and Development, 31 (2), pp. 45-66.

Ghosal, A. 2010. Robotics: Fundamental concepts and analysis, Journal of Rehabilitation and Development New Delhi, India.

Marxent. 2015. https://www.marxentlabs.com/what-is-virtual-reality/ [Accessed 02 July 2018].

Onyango, O., Daachi, B., Hamam, Y., Djouani, K. 2018. Behaviour Modelling and System Control with Human in the Loop, Simulation Modelling Practice and Theory.

Sabatini, A.M. 2002. A Mobility Aid for the Support to Walking and Object Transportation of People with Motor Impairment, Journal of Rehabilitation and Development, Lausanne, Switzerland.

Siegwart, R., Nourbakhsh, I. 2004. Autonomous Mobile Robots, 2nd Edition, Massachusetts: The MIT Press.

Smit, P.E. 2010. Development of a 3-DOF Motion Simulator Platform Master of Science in Engineering, Stellenbosch University.

Steyn, N., Hamam, Y., Monacelli, E., Djouani, K. 2014. 'Modelling and design of an augmented reality differential drive mobility aid in an enabled environment, Simulation Modelling Practice and Theory, Elsevier. https://doi.org/10.1016/j.simpat.2014.11.006.

Stroke Sleeve Spatially Distributed Tactile Feedback for Stroke Rehabilitation, http://haptics.seas.upenn.edu/index.php/Research/TactileFeedbackForRehabilitation. [Accessed 11 October 2018].

The Virtual Reality Training Facility, https://eng.sheba.co.il/virtual_reality_training_facility [Accessed 11 October 2018].